Pulmonary post-mortem findings in a series of COVID-19 cases from northern Italy: a two-centre descriptive study

Luca Carsana, Aurelio Sonzogni, Ahmed Nasr, Roberta Simona Rossi, Alessandro Pellegrinelli, Pietro Zerbi, Roberto Rech, Riccardo Colombo, Spinello Antinori, Mario Corbellino, Massimo Galli, Emanuele Catena, Antonella Tosoni, Andrea Gianatti, Manuela Nebuloni

Summary

Background **COVID-19 is characterised by respiratory symptoms, which deteriorate into respiratory failure in a substantial proportion of cases, requiring intensive care in up to a third of patients admitted to hospital. Analysis of the pathological features in the lung tissues of patients who have died with COVID-19 could help us to understand the disease pathogenesis and clinical outcomes.**

Methods **We systematically analysed lung tissue samples from 38 patients who died from COVID-19 in two hospitals in northern Italy between Feb 29 and March 24, 2020. The most representative areas identified at macroscopic examination were selected, and tissue blocks (median seven, range five to nine) were taken from each lung and fixed in 10% buffered formalin for at least 48 h. Tissues were assessed with use of haematoxylin and eosin staining, immunohistochemical staining for inflammatory infiltrate and cellular components (including staining with antibodies against CD68, CD3, CD45, CD61, TTF1, p40, and Ki-67), and electron microscopy to identify virion localisation.**

Findings **All cases showed features of the exudative and proliferative phases of diffuse alveolar damage, which included capillary congestion (in all cases), necrosis of pneumocytes (in all cases), hyaline membranes (in 33 cases), interstitial and intra-alveolar oedema (in 37 cases), type 2 pneumocyte hyperplasia (in all cases), squamous metaplasia with atypia (in 21 cases), and platelet–fibrin thrombi (in 33 cases). The inflammatory infiltrate, observed in all cases, was largely composed of macrophages in the alveolar lumina (in 24 cases) and lymphocytes in the interstitium (in 31 cases). Electron microscopy revealed that viral particles were predominantly located in the pneumocytes.**

Interpretation **The predominant pattern of lung lesions in patients with COVID-19 patients is diffuse alveolar damage, as described in patients infected with severe acute respiratory syndrome and Middle East respiratory syndrome coronaviruses. Hyaline membrane formation and pneumocyte atypical hyperplasia are frequent. Importantly, the presence of platelet–fibrin thrombi in small arterial vessels is consistent with coagulopathy, which appears to be common in patients with COVID-19 and should be one of the main targets of therapy.**

Funding **None.**

Lancet Infect Dis 2020

Published Online
June 8, 2020
https://doi.org/10.1016/S1473-3099(20)30434-5

See Online/Comment
https://doi.org/10.1016/S1473-3099(20)30449-7

Pathology Unit (L Carsana MD, R S Rossi MD, A Pellegrinelli MD, P Zerbi MD, A Tosoni BSc, Prof M Nebuloni MD), **Department of Anaesthesiology and Intensive Care Unit** (R Rech MD, R Colombo MD, E Catena MD), **and Department of Infectious Diseases** (Prof S Antinori MD, M Corbellino MD, Prof M Galli MD), **Luigi Sacco Hospital, Milan, Italy; Department of Pathology, Papa Giovanni XXIII Hospital, Bergamo, Italy** (A Sonzogni MD, A Nasr MD, A Gianatti MD); **Department of Pathology, University of Milano-Bicocca, Milan, Italy** (A Nasr); **and Department of Biomedical and Clinical Sciences, University of Milan, Milan, Italy** (P Zerbi, Prof S Antinori, Prof M Galli, Prof M Nebuloni)

Correspondence to:
Prof Manuela Nebuloni, Pathology Unit, Luigi Sacco Hospital, University of Milan, 20157 Milan, Italy
manuela.nebuloni@unimi.it

Introduction

Since the earliest reports of cases in China in December, 2019, countries around the world have faced outbreaks of COVID-19, the disease caused by the novel coronavirus severe acute respiratory syndrome coronavirus 2 (SARS-CoV-2). Italy was the first country in Europe to document a large number of cases of COVID-19, and Lombardy in particular was severely affected, with a total of 17 713 people testing positive for SARS-CoV-2 and 1593 admitted to intensive care units between Feb 20 and March 18, 2020.[1] Luigi Sacco Hospital in Milan and Papa Giovanni XXIII Hospital in Bergamo were the first hospitals in Lombardy faced with managing the epidemic crisis.

SARS-CoV-2 is the seventh member of the coronavirus family identified to cause disease in humans. Coronaviruses are enveloped, positive-sense, single-stranded RNA viruses.[2] Two other members of this family, severe acute respiratory syndrome coronavirus (SARS-CoV) and Middle East respiratory syndrome coronavirus (MERS-CoV), cause acute diffuse alveolar damage, pneumocyte hyperplasia, and interstitial pneumonia.[2–4]

At the mild end of the clinical spectrum, COVID-19 can be asymptomatic or manifest as mild upper respiratory disease with fever and cough, while severe cases can result in pneumonia, leading to acute respiratory distress syndrome (ARDS) in around 15% of hospitalised patients.[5] To the date of our last literature review (May 3, 2020), the only published reports of the pathological features of COVID-19 lung involvement were from small case series or isolated cases, both from China and other countries. In those reports, the main histological features comprised exudative diffuse alveolar damage with massive capillary congestion, often accompanied by microthrombi.[6–9]

We describe the lung histopathological findings from a large series of patients who died from COVID-19 in northern Italy, with the aim of reporting the main

Research in context

Evidence before this study

We searched PubMed up to May 3, 2020, using the search terms "autopsy" and "COVID-19", with no language restrictions. The search revealed ten reported cases. Lung morphological features of COVID-19 in deceased patients were described in a few isolated case reports and in small case series, including some reports in Chinese. Histological descriptions of lung pathology were extremely concise, without any analytical report of morphological details, and lacking any highlighting of distinctive lesions compared with other forms of interstitial pneumonia. Furthermore, as only quantitative and aggregate data were available, the possible clinical implications of the findings could not be determined.

Added value of this study

We histologically examined the lung tissues of 38 patients who died from COVID-19—to our knowledge the largest post-mortem series so far reported—in two main hospitals providing care to patients with progressive breathing failure in a peak epidemic area in Italy. We focused on the detailed analysis of histological features in these patients to elucidate any distinctive lesions associated with COVID-19. To our knowledge, these data represent the first relevant provisional information regarding tissue damage specifically induced by severe acute respiratory syndrome coronavirus 2 (SARS-CoV-2), besides the previously described diffuse alveolar damage, a feature that characterises interstitial pneumonia regardless of infectious agent.

Implications of all the available evidence

Although our observations are provisional, they were obtained in a large cohort of patients and revealed that histopathological lung damage was characterised by expected features of diffuse alveolar damage, as well as diffuse thrombotic vascular involvement. This latter finding could be relevant in the management and targeted treatment of patients infected with SARS-CoV-2, with the potential to modify outcomes.

microscopic pulmonary lesions associated with SARS-CoV-2 infection and severe respiratory failure.

Methods

Patient samples

We histologically analysed lung tissue samples from 38 consecutive patients who died from COVID-19 between Feb 29 and March 24, 2020, in two referral centres for the management of the COVID-19 outbreak in northern Italy: Luigi Sacco Hospital in Milan (20 autopsies) and Papa Giovanni XXIII Hospital in Bergamo (18 autopsies). All patients had SARS-CoV-2 infection confirmed by real-time PCR analysis of throat swab samples taken at the time of hospital admission, and all had undergone molecular tests for common respiratory viruses and bacteria by the microbiology laboratories at the respective hospitals, with negative results.

The ethics committees of Luigi Sacco Hospital and Papa Giovanni XXIII Hospital approved the use of personal and sensitive patient data for scientific research related to the disease in this study. The study followed the Italian general rules used for scientific research purposes (regulation n.72–26/03/2012).

Autopsies and tissue processing

Autopsies were done in airborne infection isolation autopsy rooms, with personnel using personal protective equipment in accordance with the Italian recommendations.[10] A team of pathologists (LC, AS, AN, RSR, AP, PZ, AG, and MN) with extensive experience in the field of infectious diseases was involved in the autopsy procedures in both hospitals.

A median of seven tissue blocks (range five to nine) were taken from each lung, selecting the most representative areas identified at macroscopic examination. Tissues were fixed in 10% buffered formalin for at least 48 h. Paraffin-embedded sections of 3-µm thickness were stained with haematoxylin and eosin. To better characterise the inflammatory infiltrate, immunohistochemical staining was done on the most representative areas of randomly selected cases, and included staining with antibodies against CD45 (clones 2B11 and PD7/26) for the identification of leucocytes, CD3 (clone 2GV6) for T lymphocytes, CD68 (clone KP-1) for monocytes, and CD61 (clone 212) for megakaryocytes. Tissues were also stained with antibodies against TTF1 (clone 8G7G2/1) and p40 (clone BC28) to identify squamous metaplasia of pneumocytes, and Ki-67 (MIB-1) to determine the proliferative index of epithelial cells. All antibodies were ready-to-use monoclonal antibodies (Ventana, Roche Diagnostics, Basel, Switzerland) and staining was done with the BenchMark Ultra IHC/ISH System (Roche, Basel, Switzerland) in accordance with the standard protocols supplied by the manufacturer. Masson trichome staining was applied to characterise collagen and fibrin deposition, epithelial cells, and fibrosis. Additionally, in cases with histological suspicion for bacterial or fungal infections, periodic acid–Schiff staining and Grocott methenamine silver staining were done to confirm morphological findings.

Additional samples from ten consecutive cases were assessed for the presence of viral particles with use of electron microscopy: two samples from each lobe were selected, fixed in glutaraldehyde, and examined with use of a Zeiss EM-109 transmission electron microscope (Zeiss, Cologne, Germany) and an Olympus MegaView G2 transmission electron microscopy camera with an integrated imaging platform (iTEM; Olympus, Munich, Germany)

Histopathological evaluation

Histological evaluation was done independently by two pathologists from each hospital, from the same team involved with the autopsy, who were masked to patient characteristics, symptoms, and diagnoses. Each pathologist analysed all the slides from both hospitals, and any discrepant results were jointly reviewed. The histological features of cellular and interstitial damage were described and graded on a semiquantitative scale on the basis of the percentage of tissue involved: absent (0%), rare (<5%), focal (5–25%), multifocal (26–50%), plurifocal (51–75%), or diffuse (>75%).[11] To quantify pulmonary intracapillary megakaryocytes, each tissue sample was scanned at low magnification to identify the hotspot area in which megakaryocytes were most easily recognisable, and CD61-positive cells in these areas were counted. A high value was defined as the presence of more than four CD61-positive cells per 25 high-power fields, which is considered to be the average number of intracapillary megakaryocytes in the lungs of people without diffuse alveolar damage.[12]

Role of the funding source

This study had no funding source. The corresponding author had full access to all the data in the study and had final responsibility for the decision to submit for publication.

Results

Patients were 33 men and five women, with a mean age of 69 years (SD 12; range 32–86). Time spent in the intensive care unit or intermediate medical ward (subintensive care) ranged from 1 day to 23 days (mean 7 days [SD 6]). Regarding past comorbidities, data were available for 31 patients: nine (29%) had diabetes, 18 (58%) had hypertension, four (13%) had past malignancies, 11 (35%) had cardiovascular disorders, and three (10%) had mild chronic obstructive pulmonary disorders. At the time of hospitalisation, all patients had clinical and radiological features of interstitial pneumonia. Of the 26 patients with available D-dimer results, all had high values (>10×the upper reference limit). Mean time from symptom onset to death was 16 days (SD 6; range 5–31).

Upon macroscopic examination, the lungs of all patients were heavy, congested, and oedematous, with patchy involvement. In all cases, histological examination revealed features corresponding to the exudative and early or intermediate proliferative phases of diffuse alveolar damage (figure 1). These features were also focally associated with patterns of interstitial pneumonia (presence of inflammatory lymphomonocytic infiltrate along the slightly thickened interalveolar septa), organising pneumonia (alveolar loose plugs of fibroblastic tissue), and acute fibrinous organising pneumonia (some alveolar spaces containing granulocytes and fibrin, with the formation of balloon structures). Features indicative of the fibrotic phase of diffuse alveolar damage, such as mural fibrosis and microcystic honeycombing, were observed to be focal, suggesting that none of the patients had progressed to the fibrotic phase, possibly because of the short duration of the disease.

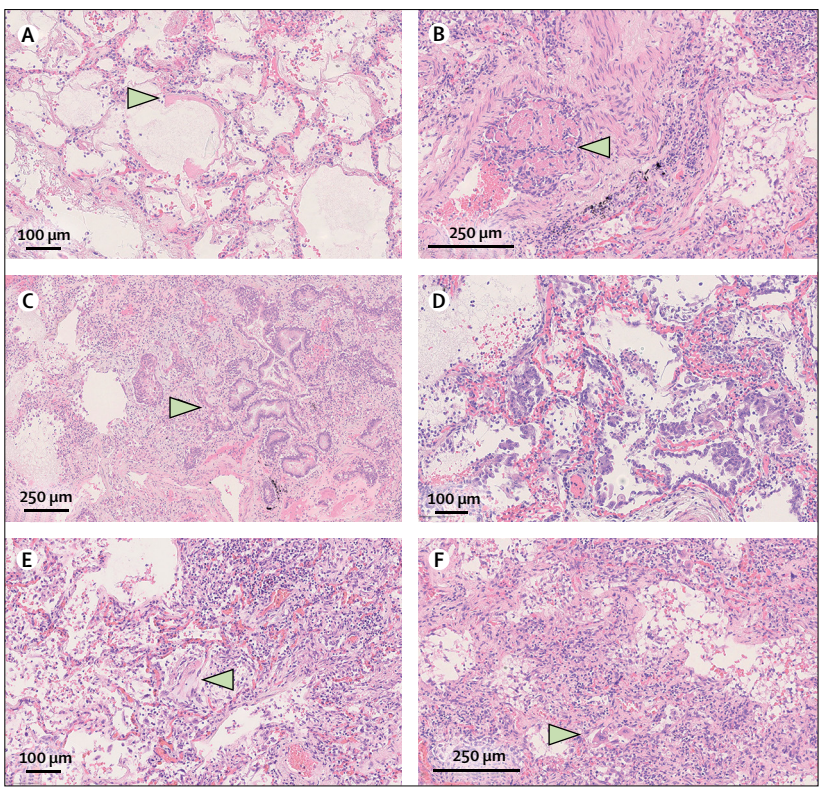

Figure 1: **Haematoxylin and eosin-stained sections from representative areas of lung parenchyma with diffuse alveolar damage**

(A) Exudative phase of diffuse alveolar damage with hyaline membranes (arrow). (B) Organising microthrombus (arrow). (C) Concomitant interstitial pneumonia, intra-alveolar scattered multinucleated giant cells (top, left), and outstanding epithelial proliferation around a bronchiole with plurifocal squamous differentiation and mild atypia (arrow). (D) Early proliferative phase of diffuse alveolar damage with many hyperplastic, and rarely atypical, type 2 pneumocytes. (E) Intermediate phase of diffuse alveolar damage with initial organising aspects (arrow) and interstitial pneumonia with marked lymphocytic infiltrate. (F) Advanced proliferative phase of diffuse alveolar damage with interstitial myofibroblastic reaction, diffuse lymphocytic interstitial infiltrate, and residual scattered hyperplastic type 2 pneumocytes (arrow). (A, D, E) Original magnification×20. (B, C, F) Original magnification×10.

Histological examination of the main bronchi and bronchiolar branches revealed mild, non-specific alterations: focal squamous metaplasia and mild transmural lymphocytic and monocytic infiltrates. Lumina often contained residual dense mucoid material, and granulocytes were present in ten cases.

Four (11%) patients also had bacterial abscesses (one or two per lung, <5 mm in diameter), and one (3%) had a single fungal abscess (<7 mm in diameter). The abscesses were presumed to have formed after hospital admission.

Morphological findings and their corresponding semi-quantitative grades are reported in the table. The predominant histological pattern of the exudative phase of diffuse alveolar damage, which was observed in all cases, included capillary congestion, interstitial and intra-alveolar oedema, dilated alveolar ducts and collapsed

	Absent	Rare	Focal	Multifocal	Plurifocal	Diffuse
Main morphological aspects						
Capillary congestion	0	0	0	24 (63%)	1 (3%)	13 (34%)
Interstitial and intra-alveolar oedema	1 (3%)	0	19 (50%)	10 (26%)	5 (13%)	3 (8%)
Alveolar haemorrhage	5 (13%)	1 (3%)	20 (53%)	8 (21%)	2 (5%)	2 (5%)
Hyaline membranes	5 (13%)	1 (3%)	19 (50%)	5 (13%)	3 (8%)	5 (13%)
Dilated alveolar ducts plus collapsed alveoli	2 (5%)	0	16 (42%)	18 (47%)	2 (5%)	0
Endothelial necrosis	9 (24%)	1 (3%)	7 (18%)	21 (55%)	0	0
Increased megakaryocytes	5 (13%)*	0	25 (66%)	4 (11%)	3 (8%)	1 (3%)
Alveolar granulocytes	6 (16%)	1 (3%)	14 (37%)	14 (37%)	2 (5%)	1 (3%)
Loss of pneumocytes	0	0	11 (29%)	20 (53%)	3 (8%)	4 (11%)
Platelet–fibrin thrombi	5 (13%)	0	16 (42%)	4 (11%)	13 (34%)	0
Type 2 pneumocyte hyperplasia with epithelial atypia	0	0	14 (37%)	9 (24%)	8 (21%)	7 (18%)
Squamous metaplasia with atypia	17 (45%)	1 (3%)	12 (32%)	7 (18%)	1 (3%)	0
Interstitial myofibroblast reaction	13 (34%)	0	18 (47%)	6 (16%)	1 (3%)	0
Alveolar granulation tissue	16 (42%)	1 (3%)	13 (34%)	3 (8%)	4 (11%)	1 (3%)
Septal collagen deposition	23 (61%)	0	13 (34%)	1 (3%)	1 (3%)	0
Alveolar loose plugs of fibroblastic tissue	27 (71%)	1 (3%)	7 (18%)	3 (8%)	0	0
Capillary proliferation	20 (53%)	0	14 (37%)	3 (8%)	0	1 (3%)
Organised alveoli plus dilated alveolar ducts	29 (76%)	0	6 (16%)	3 (8%)	0	0
Pleural involvement	38 (100%)	0	0	0	0	0
Mural fibrosis	14 (37%)	0	12 (32%)	10 (26%)	1 (3%)	1 (3%)
Microcystic honeycombing	23 (61%)	0	9 (24%)	6 (16%)	0	0
Further associated lesions						
Interstitial inflammatory infiltrate	7 (18%)	0	5 (13%)	12 (32%)	10 (26%)	4 (11%)
Alveolar inflammatory infiltrate (macrophages)	14 (37%)	1 (3%)	13 (34%)	8 (21%)	0	2 (5%)
Alveolar multinucleated giant cells	19 (50%)	6 (16%)	9 (24%)	1 (3%)	1 (3%)	2 (5%)

Tissues were categorised on the basis of the percentage of tissue involved, as follows: absent (0%), rare (<5%), focal (5–25%), multifocal (26–50%), plurifocal (51–75%), or diffuse (>75%). *Absent was defined as fewer than four cells per 25 high-power fields.

Table: **Lung histological findings in patients who died from COVID-19 (n=38)**

alveoli, hyaline membranes composed of serum proteins and condensed fibrin, and loss of pneumocytes (figure 1). Platelet–fibrin thrombi in small arterial vessels (<1 mm diameter) were found in 33 (87%) cases. Moreover, type 2 pneumocyte hyperplasia, showing various aspects of cellular atypia, was present to some extent in all patients; interstitial myofibroblastic reaction was observed in 25 (66%) cases and alveolar granulation tissue in 22 cases (58%), whereas septal collagen deposition was found in 15 (39%) cases and alveolar loose plugs of fibroblastic tissue in 11 (29%). Mural fibrosis was sometimes observed (24 [63%] cases), as was microcystic honeycombing (15 [39%] cases, most often with a focal pattern of distribution). Although no clinical history of pre-existing fibrosing interstitial lung diseases was found in patients with mural fibrosis and microcystic honeycombing, the presence of mild fibrotic alterations not in continuum with other pre-fibrotic features (myofibroblastic proliferation or organising pneumonia), as expected in a context of disease progression, might suggest that fibrosing interstitial lung diseases were pre-existing in some cases.

The inflammatory component was represented by CD45-positive and CD3-positive lymphocytes infiltrating the interstitial space; a large number of CD68-positive macrophages were also found, mainly localised in the alveolar lumina. Immunohistochemistry with anti-CD61 antibodies identified an increased number of megakaryocytes in the lung capillaries in 33 (87%) cases.

Ultrastructural examination (figure 2) revealed particles suggestive of viral infection in nine (90%) of the ten cases analysed. The particles had a mean diameter of about 82 nm and projection of about 13 nm in length. The particles, assumed to be virions, were mainly localised along plasmalemmal membranes and within cytoplasmic vacuoles, as described for other coronaviruses.[13] Infected cells were type 1 and type 2 pneumocytes; however, in two cases, particles were observed in alveolar macrophages, albeit scarcely. No particles resembling viruses were observed in multinucleated cells. Ultrastructural analyses of alveolar capillaries frequently showed platelet and fibrin plugs within the lumina, but no particles resembling virions were detected in endothelial cells.

Discussion

To our knowledge, we report the largest series of COVID-19 autopsies focusing on pulmonary lesions. In all samples, a diffuse pattern of exudative and early proliferative phases of diffuse alveolar damage was

found, while the fibrotic phase was rarely observed. The distinctive histopathological findings were atypical pneumocytes (reactive atypia) and diffuse thrombosis of the peripheral small vessels.

SARS-CoV, MERS-CoV, and SARS-CoV-2 infections show many similarities in clinical presentation.[2] SARS-CoV and MERS-CoV particles have been observed and described in pneumocytes, macrophages, and lung interstitial cells by electron microscopy, immunohistochemistry, and in situ hybridisation.[3,4,11,14] In two autopsy studies of patients who died from SARS (eight cases from Singapore[11] and 20 cases from Toronto),[3] the predominant pattern of lung injury was diffuse alveolar damage, including the exudative and proliferative phases. Inflammatory infiltrate, oedema, pneumocyte hyperplasia, fibrinous exudate, and organisation were found. The Toronto case series[3] included a comparison group of matched control patients who presented with respiratory symptoms and signs, died in the same period as those with SARS, and were negative for SARS-CoV. Compared with non-SARS lung lesions, SARS lesions were distinguishable by a prominence of vascular endothelial injury and extensive acute lung injury in varying stages of exudation and organisation.[3]

Autopsy studies of patients who died from MERS are limited. In the only complete report available,[4] the authors described lung injury characterised by exudative diffuse alveolar damage, pneumocyte hyperplasia, and septal inflammatory infiltrate.

Despite the relevance of lung involvement in patients with COVID-19, few data regarding lung pathology are available. In a case report of a patient who died from COVID-19 in China, the histological findings in the lungs included desquamation of pneumocytes, diffuse alveolar damage, and oedema.[7] In addition, Tian and colleagues[9] described the pulmonary pathology of early-phase COVID-19 in two patients with lung carcinoma; both patients showed signs of the exudative phase of diffuse alveolar damage.

In our study, fibrin thrombi in the small arterial vessels (<1 mm diameter) were observed in 87% of cases, around half of which had involvement of more than 25% of the lung tissue as well as high levels of D-dimers in the blood. These findings might explain the severe hypoxaemia that characterises ARDS in patients with COVID-19.[1] Vascular microthrombi are often identified in areas of diffuse alveolar damage, and are associated with diffuse endothelial damage. These features, although not pathognomonic, were frequent in our series, widespread in the lung samples of the patients examined, and the predominant distinctive vascular component.

Our data support the hypothesis proposed in clinical studies[15] that COVID-19 is complicated by coagulopathy and thrombosis. Furthermore, D-dimer values of greater than 1 µg/mL have been associated with fatal outcomes in patients with COVID-19.[16] For these reasons, the use of anticoagulants has been suggested to be potentially beneficial in patients with severe COVID-19, owing also to their anti-inflammatory properties, although their efficacy and safety are being closely monitored.[17–19]

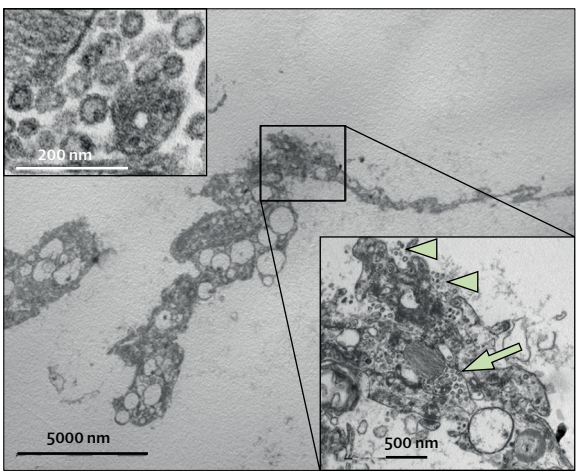

Figure 2: **Electron microscopy of a representative case**
Flat type 2 pneumocyte without lamellar electron-dense bodies of surfactant free in the alveolar space, containing numerous virions (inset bottom right) in cytoplasmic vacuoles (arrow) and along the plasma membrane (arrow heads). Virions had an average diameter of 82 nm, and viral projection about 13 nm in length (inset upper left, original magnification × 85 000).

In this study, we looked for virions in a subset of patients, and found particles resembling virions to be present, albeit rarely, in the cytoplasm of pneumocytes and macrophages. The morphology of the observed particles (about 80 nm in diameter, enveloped, with spike-like projections, and an electron-lucent core with peripheral electron-dense granules of the sectioned nucleocapsid) and their intravacuolar cytoplasmic location are consistent with the reported ultrastructural features of coronaviruses, including SARS-CoV-2.[20] Despite the low number of cases assessed, these findings might suggest that the virus remains in the lung tissue for many days, even if in small quantities, and might trigger the mechanism that leads to lung damage and causes it to progress. Further histological and molecular analyses and extension of the case series are ongoing to better define the cellular and tissue distribution of the virus as well as inflammatory responses in different organs.

Although this report represents the largest European study of lung autopsy findings from cases of COVID-19 to date and is based on the analysis of a large number of lung samples, it is limited by the absence of controls. Future pathological studies should include an extensive analysis of cases of ARDS associated with other viral pneumonias.

Contributors

LC, AS, AN, RSR, AP, PZ, AG, and MN did the autopsies and histological and ultrastructural evaluations. RR, RC, SA, MC, MG, and EC provided clinical data. AT and MN performed electron microscopy. MN, AS, LC, RC, and SA drafted the manuscript. All authors approved the final submitted version of the manuscript.

Declaration of interests

We declare no competing interests.

References

1 Grasselli G, Zangrillo A, Zanella A, et al. Baseline characteristics and outcomes of 1591 patients infected with SARS-CoV-2 admitted to ICUs of the Lombardy region, Italy. *JAMA* 2020; **323:** 1574–81.

2 Liu J, Zheng X, Tong Q, et al. Overlapping and discrete aspects of the pathology and pathogenesis of the emerging human pathogenic coronaviruses SARS-CoV, MERS-CoV, and 2019-nCoV. *J Med Virol* 2020; **92:** 491–94.

3 Hwang DM, Chamberlain DW, Poutanen SM, Low DE, Asa SL, Butany J. Pulmonary pathology of severe acute respiratory syndrome in Toronto. *Mod Pathol* 2005; **18:** 1–10.

4 Alsaad KO, Hajeer AH, Al Balwi M, et al. Histopathology of Middle East respiratory syndrome coronavirus (MERS-CoV) infection—clinicopathological and ultrastructural study. *Histopathology* 2018; **72:** 516–24.

5 Huang C, Wang Y, Li X, et al. Clinical features of patients infected with 2019 novel coronavirus in Wuhan, China. *Lancet* 2020; **395:** 497–506.

6 Barton LM, Duval EJ, Stroberg E, Ghosh S, Mukhopadhyay S. COVID-19 autopsies, Oklahoma, USA. *Am J Clin Pathol* 2020; **153:** 725–33.

7 Xu Z, Shi L, Wang Y, et al. Pathological findings of COVID-19 associated with acute respiratory distress syndrome. *Lancet Respir Med* 2020; **8:** 420–22.

8 Zhang H, Zhou P, Hu M, et al. Histopathologic changes and SARS-CoV-2 immunostaining in the lung of a patient with COVID-19. *Ann Inter Med* 2020; **172:** 629–32.

9 Tian S, Hu W, Niu L, Liu H, Xu H, Xiao SY. Pulmonary pathology of early-phase 2019 novel coronavirus (COVID-19) pneumonia in two patients with lung cancer. *J Thorac Oncol* 2020; **15:** 700–04.

10 Fineschi V, Aprile A, Aquila I, et al. Management of the corpse with suspect, probable or confirmed COVID-19 respiratory infection—Italian interim recommendations for personnel potentially exposed to material from corpses, including body fluids, in morgue structures and during autopsy practice. *Pathologica* 2020; published online March 26. DOI:10.32074/1591-951X-13–20.

11 Franks T, Chong P, Chui P, et al. Lung pathology of severe acute respiratory syndrome (SARS): a study of 8 autopsy cases from Singapore. *Hum Pathol* 2003; **34:** 743–48.

12 Mandal RV, Mark EJ, Kradin RL. Megakaryocytes and platelet homeostasis in diffuse alveolar damage. *Exp Mol Pathol* 2007; **83:** 327–31.

13 Stertz S, Reichelt M, Spiegel M, et al. The intracellular sites of early replication and budding of SARS-coronavirus. *Virology* 2007; **361:** 304–15.

14 Shieh WJ, Hsiao CH, Paddock CD, et al. Immunohistochemical, in situ hybridization, and ultrastructural localization of SARS-associated coronavirus in lung of a fatal case of severe acute respiratory syndrome in Taiwan. *Hum Pathol* 2005; **36:** 303–09.

15 Klok FA, Kruip MJHA, van der Meer NJM, et al. Incidence of thrombotic complications in critically ill ICU patients with COVID-19. *Thromb Res* 2020; published online April 10. DOI:10.1016/j.thromres.2020.04.013.

16 Zhou F, Yu T, Du R, et al. Clinical course and risk factors for mortality of adult inpatients with COVID-19 in Wuhan, China: a retrospective cohort study. *Lancet* 2020; **395:** 1054–62.

17 Tang N, Bai H, Chen X, Gong J, Li D, Sun Z. Anticoagulant treatment is associated with decreased mortality in severe coronavirus disease 2019 patients with coagulopathy. *J Thromb Haemost* 2020; **18:** 1094–99.

18 Camprubí-Rimblas M, Tantinyà N, Bringué J, Guillamat-Prats R, Artigas A. Anticoagulant therapy in acute respiratory distress syndrome. *Ann Transl Med* 2018; **6:** 36.

19 Kollias A, Kyriakoulis KG, Dimakakos E, et al. Thromboembolic risk and anticoagulant therapy in COVID-19 patients: emerging evidence and call for action. *Br J Haematol* 2020; published online April 18. DOI:10.1111/bjh.16727.

20 Ogando NS, Dalebout TJ, Zevenhoven-Dobbe JC, et al. SARS-coronavirus-2 replication in Vero E6 cells: replication kinetics, rapid adaptation and cytopathology. *bioRxiv* 2020; published online April 20. DOI:10.1101/2020.04.20.049924 (preprint).